Journal of Superhard Materials
Vol. 21, No. 3, pp. 36–48, 1999

Sverkhtverdye Materialy
No. 3, pp. 39–51, 1999
UDC 539.374:539.893

REGULARITIES OF PHASE TRANSFORMATIONS AND PLASTIC STRAINING OF MATERIALS IN COMPRESSION AND SHEAR ON DIAMOND ANVILS: EXPERIMENTS AND THEORY

N. V. Novikov[1], S. B. Polotnyak[1], L. K. Shvedov[1], and V. I. Levitas[2]

[1]*V. N. Bakul Institute for Superhard Materials of the National Academy of Sciences of Ukraine, Kiev;*
[2]*Institute of Building and Computational Mechanics, Hannover, Germany*

Regularities of phase transformations (PT) and plastic straining of materials in compression and shear in a shear high-pressure apparatus with diamond anvil cells (SDAC) have been experimentally studied and an analytical model of material phase transformations in straining between diamond anvils has been developed. Based on a higher yield stress of a new phase and an additional plastic flow of the specimen material from the center to its periphery, we have offered a new explanation of the pressure self-multiplication phenomenon occurring in phase transformations. The rotation of the anvil contributes to the production of fundamentally new materials that cannot be produced by compression without rotation. If two materials which differ only in the yield stress form due to phase transformations, then a material having a lower yield stress forms in compression without rotation, while a harder phase forms in compression with rotation. Therefore, the method based on the material compression with rotation is of particular importance for producing high-strength materials.

Phase transformations in elastoplastic materials are one of the most abundant phenomena in the nature, physical experiments and modern technologies. They are widely used in metallurgy, thermomechanical processing of materials, and in the production of new materials with predetermined properties, e.g., in synthesis of superhard materials. Various factors like temperature, high pressures, impurities, large plastic compression and shear deformations, etc. affect essentially the PT proceeding and the formation of the required microstructure of the material with predetermined physico-mechanical properties, thus considerably decreasing, for instance, the transformation pressure. In this case, the formation of new structures that cannot be produced without an additional plastic straining is a possibility. The majority of these phenomena have a purely qualitative explanation and their applications in technological processes are based on purely empirical regularities. The mechanics of materials under these conditions is not adequately developed. Therefore, more comprehensive studies of the effect of stresses, deformations, temperatures and high pressures on the PT proceeding should result in the development of experimentally justified theories and computer-aided models allowing for possible variations in the structure and phase states of real materials as well as in new processes and materials.

1. Experimental studies of regularities of phase transformations and plastic deformation of materials in compression and shear in a SDAC

1.1. High-pressure apparatus with diamond anvil cells. At present high-pressure apparatus with diamond anvils (DAC) are most widely used for obtaining new results in high-pressure physics, mechanics and materials science. Unique properties of diamond crystals together with the procedures for measuring pressure from a shift of the ruby fluorescence line [1] and creation of hydrostatic pressures [2] have made the DAC a perfect tool for quantitative studies of materials under extreme conditions [3, 4]. Transparency of diamond crystals allows optical diagnostics of tested specimens. For this purpose, a wide range of wave lengths in IR, visible, UV, and rigid X-ray radiations is used.

A great deal of DAC designs have been developed and used. They differ, mainly, in design of alignment and loading units. Five basic types of DAC can be distinguished [3, 4] for different research purposes. They are called by the names of their developers: Piermarini and Block (up to 50 GPa), Bassett (up to 40 GPa), Mao and Bell (above 100 GPa), Suassen-Holzapfel (up to 50 GPa) and Merrill-Bassett (up to 100 GPa). A typical schematic of the high-pressure system with diamond anvils is presented in Fig. 1. It consists of

- a high-pressure cell with diamond anvils to create pressure,
- a system for pressure measurement at room temperature,
- a system for high-temperature heating and temperature measurement,
- an opto-mechanical system for observation.

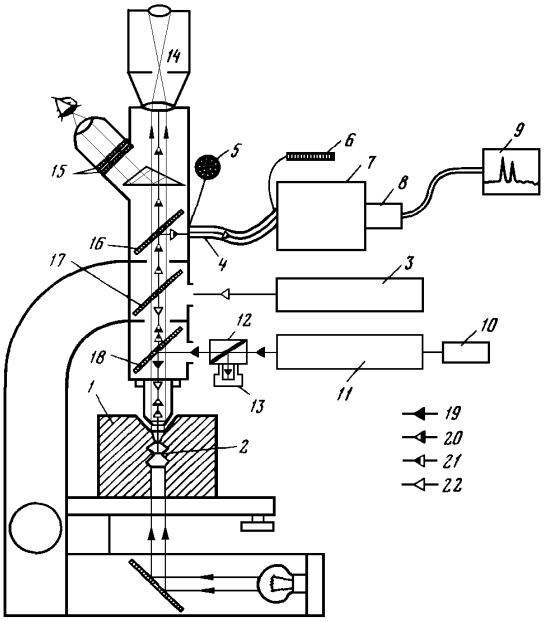

Fig. 1. Schematic diagram showing a high-pressure system with diamond anvils: *1* — DAC, *2* — specimen, *3* — laser for excitation of the ruby fluorescence, *4* — fiber-optical cable, *5* — section of the fiber-optical cable, *6* — section matching the opening of a monochromator, *7* — monochromator, *8* — photomultiplier, *9* — spectrograph, *10* — laser for aligning the optical system, *11* — laser for heating a specimen, *12* — polarizer, *13* — laser trap, *14* — optical pyrometer, *15* — filters to protect eyes against laser radiation, *16, 17, 18* — dichroic mirrors. Arrows indicate the path of rays from a laser for specimen heating (*19*), heated specimen radiation in the visual range of the spectrum (*20*), ruby fluorescence (*21*), laser for excitation of the ruby fluorescence (*22*).

A high-pressure cell with diamond anvils consists of a pair of diamond anvils-windows, an alignment unit, a piston system, a gasket with a specimen, and a loading unit. The system for pressure measurements at room temperature comprises ruby crystals in the specimen, a laser or a mercury lamp for excitation of the ruby fluorescence, a spectrometer, mirrors, and fiber-optical cables. The system for high-temperature heating and temperature measurements includes a continuous or a pulse laser, mirrors, and an optical pyrometer. The opto-mechanical system for observation includes a microscope for visual observation and control of plane-parallelism of the working faces in compression and recording devices. The recording devices involve a photographic or a motion picture cameras and videorecorder.

Apparatus with diamond anvils are space-saving (5—15 cm) and easily combined with working units of other research equipment. They ensure extremely wide ranges of pressure (from 100 kbar to 5 Mbar) and temperatures (from 0.04 K to 4000 °C). These apparatus are used to perform various researches at high pressures, e.g., for X-ray diffraction studies of compressed poly- and monocrystalline specimens; to study absorption, as well as combined, Raman and Moessbauer spectra, including those which are taken using modern spectroscopic methods and laser; to study radioactivity, superconductivity under pressure at cryogenic temperatures; for opto-microscopic structural examinations; to study elastic properties of substances, to determine ultimate strength and deformability; for various electrical measurements.

The principle of operation of the apparatus is simple. A specimen is placed between plane-parallel surfaces of two diamond anvils (Fig. 2). When the anvils approach each other under the action of an external force, high static pressures generate in the specimen.

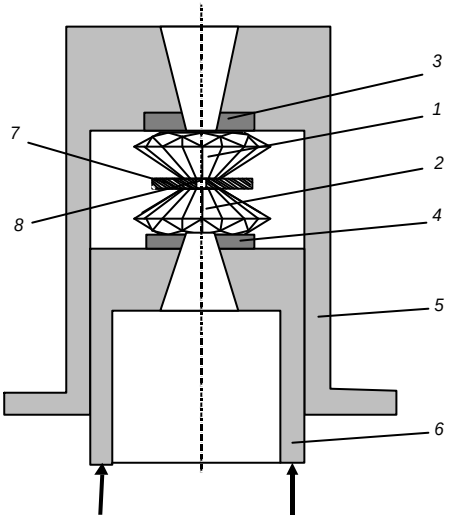

Fig. 2. Scheme of a high-pressure unit with diamond anvils: *1*, *2* — diamond anvils, *3*, *4* — supporting plates, *5* — cylinder, *6* — piston, *7* — deformable gasket, *8* — specimen.

1.2. Shear high-pressure apparatus with diamond anvils. A shear high-pressure apparatus with diamond anvils (SDAC) is a further stage in the development of experimental technique to create high pressures. This apparatus allows one to generate both a high static compression pressure in a specimen and large shear deformations in rotation of anvils relative to each other around the load axis.

Figure 3 is a schematic representation of a shear high-pressure apparatus with diamond anvils used at V. N. Bakul Institute for Superhard Materials of the National Academy of Sciences of Ukraine. The shear deformation is realized by rotation of piston *4* with a diamond anvil with respect to immovable cylinder *6* with the other diamond anvil fixed on it. The alignment of the diamond anvils such that their working surfaces coincide and set perpendicularly to the rotation

axis is realized accurate to 0.02° by two spherical bearings *5* and 16 screws, 8 of which are used to move anvils in the plane perpendicular to the load axis, while other 8 to change the slope of the anvils. An original loading unit of the second class lever type is used. It is controlled by a mechanical lever-spring system (Fig. 4) that allows a smooth adjustment of the force applied to anvils up to 4000 N. The ratio between lever arms is 5:1. Spring *2* that transmits the force to the larger arm of the lever where a high-pressure unit with a cylinder and a piston is positioned, is compressed by rotation of nut *1*. In this case, a high parallelism of the anvil working surfaces in compression is attained. A SDAC having a special-shape slit in carbide plate *2* (Fig. 3) under diamond anvil *3* permits the cell to be used for X-ray studies.

1.3. Measurement of pressure in a specimen. To measure the pressure distribution in a specimen, the method of a ruby manometer is used [1]. It allows a rapid *in situ* measurement of pressure in a DAC from the shift of the R_1 ruby fluorescence line. The essence of the method is as follows. 3—5-μm fragments of a ruby crystal are placed near the tested specimen or are applied onto its surface (without a gasket). In the course of the experiment, the argon laser excites the fluorescence of ruby. The fluorescence spectrum is recorded by a spectrophotometer and transferred to a PC. The pressure is evaluated from the shift of a wavelength of the R_1 fluorescence line (Fig. 5).

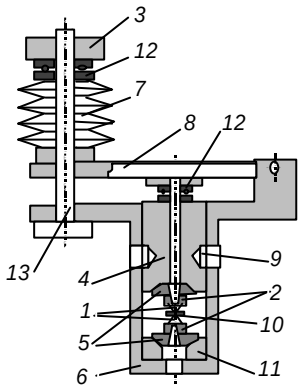

Fig. 3

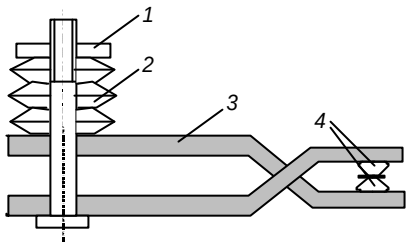

Fig. 4

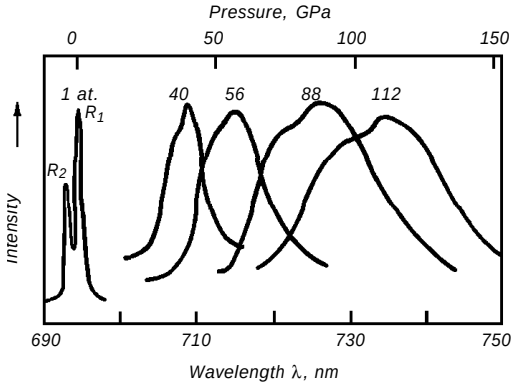

Fig. 5

Fig. 3. Scheme of a SDAC: *1* — diamond anvils, *2* — supporting plates, *3* — nut, *4* — piston, *5* — alignment supporting plates, *6* — cylinder, *7* — spring, *8* — lever, *9* — slot of a steering lever, *10* — specimen, *11* — immovable piston, *12*— bearing, *13* — screw.

Fig. 4. Scheme of a lever-type loading device: *1* — nut, *2* — spring, *3* — lever, *4* — diamond anvils.

Fig. 5. Pressure dependence of the shift of the R_1 ruby fluorescence line.

The time for pressure measurement at one point does not exceed 20 s. Pressure can be measured both at an individual point and by a two-dimensional grid using an automated system. The scanning in 600 points at a space of 10 μm takes about 3.5 h.

1.4. Studies of the effect of high pressures and shear deformations on phase transformations in potassium chloride. Potassium chloride (KCl) is an easy model material for optical studies. It is characterized by a relatively small value of pressure of the B1 → B2 polymorphic transformation (about 2 GPa), which can be observed visually. Our experiment was aimed at studying the effect of shear deformation on the pressure redistribution in phase transformation. Figure 6 shows the pressure distribution in a specimen before and after shear deformation ($\varphi = 10°$).

At the early stage of increasing loading, at the center of a disk specimen a biphase area is observed, that corresponds to the onset of transformation in compression. Near the phase boundary, the diagram (see Fig. 6) exhibits a step-like characteristic anomaly. If the phase transformation pressure has been exceeded, the shear deformation causes the redistribution of the radial pressure over the specimen, i.e. an increase of the pressure at the center and some reduction at the periphery of the specimen.

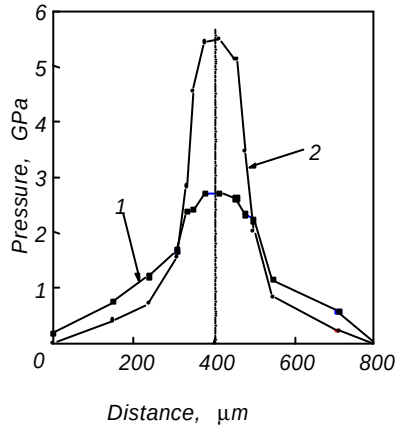

Fig. 6. Pressure distribution over the diametric section of a KCl specimen in compression (*1*) and shear by 10° (*2*) at a constant load. The center of the anvil is located at a point of 400 μm.

Thus, if a phase transformation takes place when a specimen is compressed in a SDAC, then the application of shear loads induces an essential redistribution of pressure over the specimen (the pressure self-multiplication effect).

1.5. Studies of the effect of high pressures and shear deformations on phase transformations in the C_{60} fullerene. By the term "fullerene" we mean closed molecules of C_{60}, C_{70}, C_{76}, and C_{84} types, in which all atoms of carbon are in the apices of regular hexagons or pentagons on spherical or spheroidal surfaces. The central place among fullerenes is occupied by C_{60}, that is the most symmetric and hence the most stable molecule resembling a football-cover and having a structure of a regular truncated icosahedron. Each atom of carbon in the C_{60} molecule is in apices of two hexagons and one pentagon.

Increased interest in the phase diagram of C_{60} at high pressures is related to both the attempts to define the stability limit of a fullerene molecule and the possibility to produce its high-pressure phase, whose elastic modulus, according to some assessments [5], exceeds that of diamond. The mechanism of producing a superhard phase can be as follows [5]. With increasing pressure, a decrease in the degree of symmetry in the C_{60} molecule accompanied by an enrichment of its IR spectrum may be observed, which is due to the removal of the degeneracy of those vibrations that are caused by the symmetry. In this case, of some importance are localized states caused by orientation disordering and the possibility of forming, at high pressures, a hard fullerene

structure with covalent bonds between carbon atoms of different C_{60} molecules as in the case of diamond.

At the Institute for Superhard Materials we have experimentally tested these assumptions at room temperature and a pressure of up to 22 GPa, and compared our results with those reported elsewhere [6].

Hard fullerene C_{60} was subjected to nonhydrostatic compression up to 10 GPa and 18 GPa and shear deformations in a SDAC by a rotation of one of the anvils around the load axis by an angle of 5°. In the course of the experiment the pressure distribution along the diameter of the anvil working surfaces was measured. Besides, the variation of the transmitted-light absorption coefficient of a specimen both in the visible and in the near-infrared regions of the spectrum for wavelengths of 0.9—1 μm was visually observed by an electron-optical converter. Figure 7 shows the pressure distribution along the anvil diameter. On the plot, r = 250 μm corresponds to the center of the anvil and r = 0 and r = 500 μm correspond to the periphery.

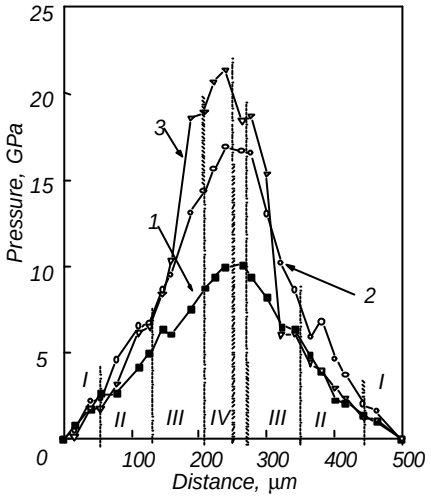

Fig. 7. Pressure distribution over the diametric section of the C_{60} fullerene specimen when compressed up to 10 (*1*) and 18 (*2*) GPa and shifted by 5° under a constant load (3).

From step-like anomalies in the pressure profiles, we have found three phase transformations. These anomalies correlate with optically observed phase boundaries as different phases of C_{60} have different coefficients of the transmitted light absorption.

Phase I. The initial C_{60} fullerene.

Phase II. At pressures of about 2 GPa, the I-II-I direct and reverse phase transformations are observed. The phase is characterized by an irregular dark-purple spot having well-defined phase boundaries when observed in the transmitted light in the visible spectrum region.

Phase III. At pressures of about 6 GPa, the II-III direct phase transformation is observed. When the pressure is released no reverse transformation is observed. The spectrum of the transmitted light absorption of the phase shifts further into the infrared region and is characterized by an appearance of a dark irregular spot visually observed in the near infrared region using an electron-optical converter.

Phase IV. At pressures of about 20 GPa after shear deformation, the nuclei of the phase as light points on a dark background are observed in the transmitted light in the near infrared region. The phase is metastable.

It should be noted that in the experiments we tried to obtain only individual nuclei of this phase and did not expected that the obtained particles can cause a local fracture of the anvil surface. The highest static pressure of compression did not exceed 18 GPa, but at the shear

deformation by an angle of about 5°, the pressure has abruptly increased up to 22 GPa and we have clearly observed the nuclei of phase IV. After unloading the SDAC, mechanical defects as cracks and individual grooves from 1 to 3 μm wide have been found on the anvil surfaces, which are well seen in the SEM micrographs from anvil surfaces (Fig. 8) (a BS340 scanning electron microscope equipped with the image analysis system was used). The initiation of the grooves and cracks on the surface of the hardest known substance, diamond, indicates that the hardness of phase IV of the fullerene C_{60} is at least no lower than that of diamond at 22 GPa.

Figure 9 shows the cathodoluminescent topogram of the working surface of the upper anvil, where the "collapses" are observed. However, a higher magnification shows that the anvil surface is smooth and does not contain any visible cracks. Its "collapses" can be induced by significant stresses under surface owing to a large density of dislocations caused by the anvil deformation.

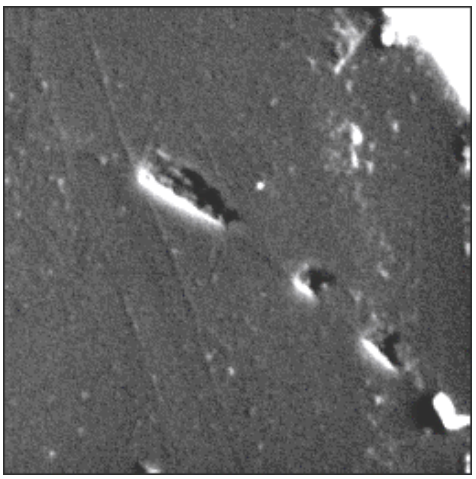

Fig. 8

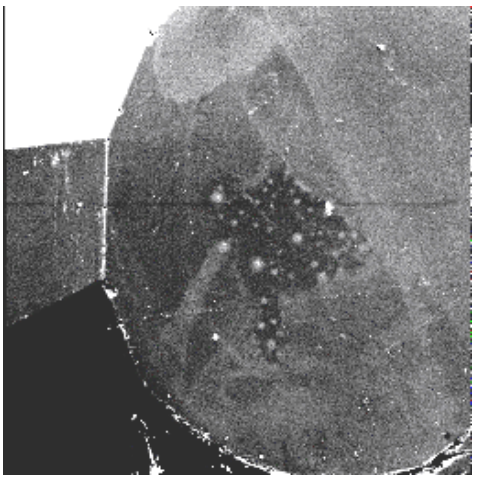

Fig. 9

Fig. 8. SEM micrograph from the diamond anvil surface with grooves formed by slipping hard C_{60} fullerene grains over anvil surface during shear (2000×).

Fig. 9. Cathodoluminescent topogram of the upper diamond anvil surface.

1.6. Study of the deformation history effect on the pressure distribution throughout a specimen material. To study the effect of the deformation history on the pressure distribution throughout a specimen material when compressed on diamond anvils, series of experiments on deformation of disk specimens of NaCl and Kh18N10T hardened stainless steel have been performed at monotonous and quasi-monotonous loadings. The initial thicknesses of the specimens were 200 μm (for NaCl) and 300 μm (for steel) and the final thicknesses 20 and 30 μm, respectively.

The following loading conditions were realized:

Specimen material	Loading conditions
NaCl	1) compression to a thickness of h = 20 μm
	2) compression — unloading — compression to h = 20 μm
	3) compression — shear by an angle of $2\varphi = 6°$ — compression to h = 20 μm
Kh18N10T steel	1) compression to a thickness of h = 30 μm
	2) compression — unloading 1 — compression to h = 30 μm
	3) compression — unloading 2 — compression to h = 30 μm.

Figures 10 and 11 show the radial pressure profiles in specimens for the above loading conditions.

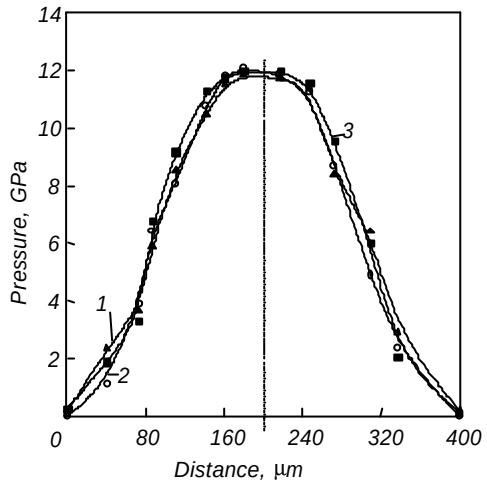

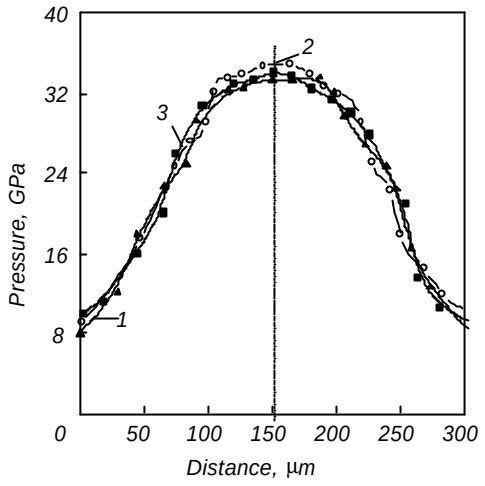

Fig. 10. Pressure distribution with diameter of the diamond anvil over a NaCl specimen under the first (*1*), second (*2*) and third (*3*) loading conditions.

Fig. 11. Pressure distribution with diameter of the diamond anvil over a Kh18N10T steel specimen under the first (*1*), second (*2*) and third (*3*) loading conditions.

The data analysis shows that the highest difference in pressure for the steel specimen is 3 GPa (9%) and for the NaCl specimen 1.2 GPa (10%). Thus, in the absence of phase transformations in the tested material, the deformation history does not essentially affect the final pressure distribution in the specimen, if the specimen deformation is large.

This regularity supports a postulate about the existence of the perfectly plastic boundary surface [7]: beginning with a certain degree of deformation, the materials deform as perfectly plastic, isotropic and homogeneous with a deformation-history-independent perfectly plastic boundary surface.

Thus, it is experimentally found, that

– an additional application of shear loads to a tested specimen at a fixed axial force intensifies the phase transformation in a specimen material, i.e. the structural transformations begin at lower pressures than in the case of the axial load only (without shear deformations);

– if the phase transformation occurs in compression of a specimen in a SDAC, the anvil rotation and hence the plastic deformation result in essential pressure redistribution in a specimen (effect of the pressure self-multiplication);

– beginning with some (rather high) level of the plastic deformation, the deformation history has no essential influence on the final pressure distribution in a specimen material. This supports a postulate about the existence of the perfectly plastic boundary surface of materials.

Besides, it has been experimentally shown in [8] that a volume fraction of a new phase in specimens depends on the shear deformation value (i.e., on the anvil rotation angle).

To explain the experimental data, we have developed a theoretical model, which describes the regularities of the material phase transformations in compression and shear on diamond anvils.

2. Theoretical investigation of the material phase transformations in compression and shear on diamond anvils

2.1. Stressed state of a thin cylindrical disk in compression and shear on anvils. Let's consider the stressed state of a thin cylindrical disk in compression and shear on anvils (Fig. 12).

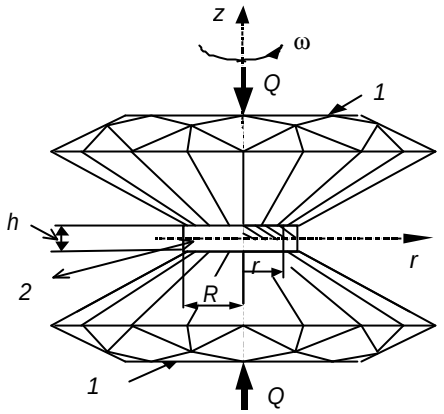

Fig. 12. Compression of a thin disk (*2*) on diamond anvils (*1*).

As the elastic deformations of the anvils and the disk are very small, we use the well-known simplified equilibrium equation [11]

$$\frac{\partial p}{\partial r} = -\frac{2\tau_r}{h}, \tag{1}$$

where r is the radial coordinate, h is the current thickness of the disk, τ_r is the radial component of the friction-induced shear stress $\mathbf{t}$ along the boundary S between the anvils and the disk. Friction-induced shear stresses $\mathbf{t}$ are directed opposite to the velocity $\mathbf{v}$ of relative sliding of the compressed material along the boundary S. For a thin disk, the modulus $\mathbf{t}$ reaches usually its maximum value equal to half the yield stress σ_Y. In the case without rotation of the anvil, $\tau_r = 0.5\sigma_Y$ and Eq. (1) yields

$$\frac{\partial p}{\partial r} = -\frac{\sigma_Y}{h} \quad ; \quad p = \sigma_0 + \sigma_Y\left(1 + \frac{R-r}{h}\right), \tag{2}$$

where $p = \sigma_0 + \sigma_Y$ is the boundary condition at the external radius of the anvil $r = R$, σ_0 is the pressure of external support of an anvil at $r = R$ due to the material extruded from the working region of the anvils at $r > R$. The applied load is determined by integration of $p(r)$ for S,

$$Q = \pi R^2\left(\sigma_0 + \sigma_Y\left(1 + \frac{R}{3h}\right)\right). \tag{3}$$

Radial component of velocity v_r is defined from the incompressibility condition and the condition that $v_r = 0$ at $r = 0$ from equation $\mathbf{v} = -\dot{h}\frac{\mathbf{r}}{h}$. In rotation of one of the anvils with an angular velocity of ω, the expression for v_r is still valid, but the circumferential velocity component $v_\theta = \omega r$ appears. In this case, the velocity vector $\mathbf{v}$ and shear stress $\tau = 0.5\sigma_Y\frac{\mathbf{v}}{|\mathbf{v}|}$ are inclined to the radius at an angle α,

$$\cos\alpha = \frac{v_r}{\sqrt{v_r^2 + v_\theta^2}} = \frac{1}{\sqrt{1 + \left(\omega \frac{h}{\dot{h}}\right)^2}} \tag{4}$$

and, respectively,

$$\tau_r = 0.5\sigma_Y \cos\alpha . \tag{5}$$

Substituting Eq. (5) into Eq. (1) yields

$$p = \sigma_0 + \sigma_Y\left(1 + \frac{R - r}{H}\right), \tag{6}$$

$$Q = \pi R^2\left(\sigma_0 + \sigma_Y\left(1 + \frac{R}{3H}\right)\right), \tag{7}$$

$$H = \frac{h}{\cos\alpha} = h\sqrt{1 + \left(\frac{\omega h}{\dot{h}}\right)^2} , \tag{8}$$

i.e. this is equivalent to substitution of h for H. Let rotation occurs at the fixed axial load Q. Then the condition Q = const with the assumption of σ_0 = const results in H = const = h_0, where h_0 is the thickness of the disk at the instant the rotation begins, and the differential equation of the disk thickness reduction is of the form

$$d\varphi := \omega\, dt = -\frac{dh}{h}\sqrt{\left(\frac{h_0}{h}\right)^2 - 1} . \tag{9}$$

Equation (9) shows that at Q = const and, hence, at H = const, the pressure distribution is independent of the anvil rotation, which agrees with the experimental data.

Consequently, the anvil rotation is equivalent to a reduction of friction in the radial direction and decreases the disk thickness and this decrease is uniquely related to the rotation angle φ.

2.2. Phase transformation in a specimen when deformed on diamond anvils. Let a PT occurs at the center of the disk (Fig. 13). We use a PT criterion for elastoplastic materials [9, 10],

$$\iiint_{\mathbf{e}_1}^{\mathbf{e}_2} \mathbf{s} : d\left(\mathbf{e}^e + \mathbf{e}^f\right)dV - \int_V \Delta\psi dV = \int_V k dV , \tag{10}$$

where **σ** is the stress tensor, **εe** and **εf** are the tensors of elastic and phase deformations, respectively, V is the nucleus volume, ψ is the specific Helmholz free energy, k is the increment of dissipation due to the phase transformation in a unit volume, $\Delta\psi = \psi_2 - \psi_1$, indices 1 and 2 indicate the phase before and after the phase transformation.

For the case of equal elastic properties of phases $\mathbf{E}_1 = \mathbf{E}_2$, where $\mathbf{E}_i$ are the tensors of elastic moduli of the i-th phase, the criterion (10) is of the form

$$\iiint_{\mathbf{e}_1}^{\mathbf{e}_2} \mathbf{s} : d\mathbf{e}^f\, dV - \int_V \Delta\psi^\theta dV = \int_V k dV , \tag{11}$$

where ψ^{θ} is the temperature component of the free energy, i.e. elastic deformations also disappear. Let us assume that shear phase deformation $\mathbf{g}^f$ equals zero, then $\mathbf{e}^f = \frac{1}{3}\mathbf{e}_0^f \mathbf{l}$, where I is the unit tensor, ε_0^f and $\mathbf{g}^f$ are the volume and shear phase deformations. In this case $\mathbf{\acute{o}}:d\mathbf{\mathring{a}}^f = pd\,\mathbf{e}_0^f$, where p is the hydrostatic pressure. As the volume phase deformation and k are constant in a nucleus, Eq. (11) can be written as

$$\int_{\varepsilon_{01}^f}^{\varepsilon_{02}^f} \overline{p} d\varepsilon_0^f - \Delta\psi^{\theta} = k, \overline{p} = \frac{1}{V}\int p dV, \tag{12}$$

where $\overline{p}$ is the pressure averaged over a nucleus.

Let c be the volume of a new phase in transformation region A. In the case of no rotation of an anvil, a part of the disk material flows to the center of the anvil. The neutral EF circle having the zero velocity of a relative sliding can be easily found using a volume balance equation. Equation (1) is valid, but shear stresses in the EF region change the sign and in the A region the yield stress σ_{Y_2} of a new phase, which depends on c, should be used. We assume that the pressure does not undergo an abrupt change at the interface.

A complete analytical solution of the problem looks rather complicated, but the results can be schematically represented as shown in Fig 13.

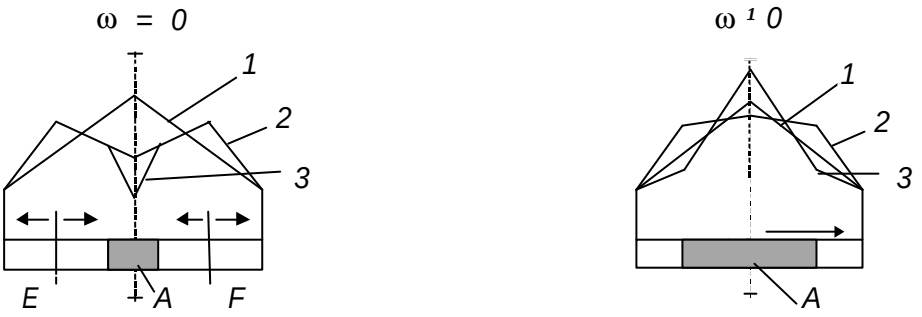

Fig. 13. Pressure distribution in a thin disk compressed on diamond anvils: (*a*) *1* — before PT, *2* — after PT at $\sigma_{Y1} = \sigma_{Y2}$, *3* — after PT at $\sigma_{Y1} < \sigma_{Y2}$; (*b*) *1* — $\sigma_{Y1} = \sigma_{Y2}$, *2* — $\sigma_{Y1} > \sigma_{Y2}$, *3* — $\sigma_{Y1} < \sigma_{Y2}$.

It should be noted that in the absence of the anvil rotation under the fixed axial force Q, the pressure in the region of transformation and the work integral in Eq. (12) decrease significantly, which impairs the PT conditions. The higher σ_{Y2}, the greater pressure reduction in the transformation region.

In the rotation of the anvil, the disk thickness and hence the variation of a negative pressure in the transforming particle decrease, which results in an increase of the work integral and the driving force for PT.

Optimal pressure variation, which satisfies the postulate of realizability [9, 10], will be in case of unlimited radial flow from the center of the disk. In this case, shear stresses do not change sign, the pressure grows monotonically with decreasing radius and a decrease in volume due to PT is fully compensated by a reduction in thickness. The last-mentioned condition in terms of Eq. (9) and at $\sigma_{Y1} = \sigma_{Y2}$ results in the differential equation

$$dc\varepsilon_0 = -\frac{dh}{h} = d\varphi\left(\left(\frac{H}{h}\right)^2 - 1\right)^{-0.5}, \quad (13)$$

which uniquely relates the variation of the volume fraction of a new phase in the PT region to the rotation angle.

For $\sigma_{Y1} \neq \sigma_{Y2}$, the equation similar to Eq. (13) looks more complicated, but it also uniquely relates the variation of the volume fraction of a new phase in the PT region to the rotation angle.

According to Eq. (1) if both the phases have the same yield stress, the pressure distribution after the PT is the same as before the PT (Fig. 13*b*). If the new phase is softer, the pressure decreases at the center, if the new phase is harder, the pressure increases at the center. Consequently, despite the volume decrease caused by the PT, the pressure increases due to the origination of a harder phase and additional plastic flow, which is in agreement with the experimental data (effect of the pressure self-multiplication).

The above solution allows us to explain why the rotation of an anvil favours the obtaining of fundamentally new materials, which cannot be obtained in compression without rotation. If two materials, which differ in the yield stress only, can form due to PT, then the material having a lower yield stress forms in compression without rotation of an anvil, and the harder phase forms under compression with rotation. Therefore, the method based on the compression of materials with rotation of anvils is especially important for the production of high-strength materials.

CONCLUSIONS

Regularities of plastic deformation and phase transformations of materials in compression and shear in diamond anvil cell (SDAC) have been experimentally studied. It has been found that

– additional shear loads applied to the tested specimen at a fixed axial force intensify the phase transformation in a specimen material, i.e. the structural transformations begin at lower pressures than in the case of axial load only (without shear deformations);

– if the phase transformation occurs in a specimen in compression in a SDAC, application of shear loads results in the essential pressure redistribution over the specimen (effect of the pressure self-multiplication);

– beginning with some (rather high) degree of plastic deformation, the deformation history has no essential influence on the final pressure distribution in a specimen material. This confirms a postulate about the existence of the perfectly plastic boundary surface of materials.

We have studied C_{60} fullerene specimens in compression and shear in a SDAC up to 22 GPa at room temperature. In case of the combination of the nonhydrostatic compression and shear deformation, the presence of the superhard phase of the C_{60} fullerene having a yield stress comparable to that of diamond has been revealed in the tested specimen.

A theoretical solution of the phase transformation problem for materials in compression and shear on diamond anvils has shown that

– the improvement of the conditions for phase transformation due to the rotation of anvils is related to the possible additional displacement, which compensates for a volume decrease at PT. This is due to a decrease in friction stress in a radial direction at the anvil rotation;

– an optimal pressure variation in the region of phase transformation will occur if the volume decrease due to PT is completely compensated for by a reduction in thickness because of the anvil rotation. This condition results in the differential equation, which relates variation in the volume fraction of the new phase in the PT region to the anvil rotation angle;

– the rotation of an anvil is much more efficient in synthesis of a harder phase than in synthesis of a soft phase. If two materials, which differ in the yield stress only, can form due to PT, then the material having a lower yield stress forms under compression without rotation of an anvil, and the harder phase forms under compression with rotation.

We have found a new explanation for the phenomenon of the pressure self-multiplication effect at PT on diamond anvils on the strength of a higher yield stress of the new phase and additional plastic flow from the specimen center to its periphery.

REFERENCES

1. G. J. Piermarini, S. Block, J. D. Barnett, and R. A. Forman, "Calibration of the pressure dependence of the R_1 ruby fluorescence line to 195 kbar," J. Appl. Phys., vol. 46, no. 6, pp. 2774—2780, 1975.

2. A. Van Valkenburg and L. S. Whatley, "High pressure optics," in: Advances in High Pressure Research, pp. 327—368, Academic Press, New York, 1966.

3. A. Jayaraman, "Diamond anvil cell and high-pressure physical investigations," Rev. Modern Phys., vol. 55, no. 1, pp. 65—108, 1983.

4. A. Jayaraman, "Ultrahigh prressure," Rev. Sci. Instrum., vol. 57, no. 6, pp. 1013—1031, 1986.

5. R. S. Ruoff and A. L. Ruoff, Nature, vol. 350, pp. 663—664, 1991.

6. V. D. Blank, M. Popov, S. G. Buga, V. Davydov, et al., "Is C_{60} fullerite harder than diamond?" Phys. Lett. A, vol. 188, pp. 281—286, 1994.

7. V. I. Levitas, Large Deformation of Materials with Complex Rheological Properties at Normal and High Pressure, Nova Science Publishers, New York, 1996.

8. V. P. Bokarev, O. M. Bokareva, I. I. Tempizky, and S. S. Batsanov, "Influence of shear deformation on phase transformations progress in BaF_2 and SrF_2," Solid State Physics, vol. 28, pp. 813— 816, 1986.

9. V. I. Levitas, "Thermomechanics of martensitic phase transformations in elastoplastic materials," Mech. Res. Commun., vol. **22**, pp. 87—94, 1995.

10. V. I. Levitas, "Theory of martensitic phase transformations in elastoplastic materials," Journal de Physique IV, Colloques C2, vol. 5, pp. 41—46, 1995.

11. P. M. Ogibalov and I. A. Kiyko, Notes on High Parameters Mechanics [in Russian], Moscow University, Moscow, 1962.

24 November 1998